

# Universal correlations in the nuclear symmetry energy, slope parameter, and curvature

Jeremy W. Holt<sup>1,2,\*</sup> and Yeunhwan Lim<sup>1,†</sup>

<sup>1</sup>*Cyclotron Institute, Texas A&M University, College Station, TX 77843, USA*

<sup>2</sup>*Department of Physics and Astronomy, Texas A&M University, College Station, TX 77843, USA*

(Dated: May 4, 2018)

From general Fermi liquid theory arguments, we derive correlations among the symmetry energy ( $J$ ), its slope parameter ( $L$ ), and curvature ( $K_{\text{sym}}$ ) at nuclear matter saturation density. We argue that certain properties of these correlations do not depend on details of the nuclear forces used in the calculation. We derive as well a global parametrization of the density dependence of the symmetry energy that we show is more reliable, especially at low densities, than the usual Taylor series expansion around saturation density. We then benchmark these predictions against explicit results from chiral effective field theory.

PACS numbers:

The nuclear isospin-asymmetry energy, which characterizes the energy cost of converting protons into neutrons in an interacting many-body system, is an important organizing concept linking the properties of atomic nuclei to the structure and dynamics of neutron stars. In particular the isospin-asymmetry energy governs the proton fraction of dense matter in beta equilibrium, the thickness of neutron star crusts, and the typical radii of neutron stars [1–6]. For these reasons the nuclear isospin-asymmetry energy is a primary focus of experimental investigations at current and next-generation rare-isotope facilities such as the Radioactive Isotope Beam Factory (RIBF), the Facility for Antiproton and Ion Research (FAIR), and the Facility for Rare Isotope Beams (FRIB).

In recent years, theoretical [6–10] and experimental [11–15] studies have reduced the uncertainties on the isospin-asymmetry energy at and below the density scales of normal nuclei, but more challenging is to derive constraints at the higher densities reached in the cores of neutron stars. Given the experimental difficulties of creating and studying high-density, low-temperature matter in the lab, an alternative strategy has been to extract the coefficients in the Taylor series expansion of the isospin-asymmetry energy about nuclear matter saturation density. For instance, the slope parameter has been shown to correlate strongly with neutron skin thicknesses in nuclei [13, 16, 17], nuclear electric dipole polarizabilities [18–23], and the difference in charge radii of mirror nuclei [24, 25]. Determining the isospin-asymmetry energy curvature is more challenging [26–28] with larger associated uncertainties.

A feature observed in many experimental and theoretical investigations is a nearly linear correlation between the value of the isospin-asymmetry energy at nuclear matter saturation density, its slope, and curvature (for a recent comprehensive analysis, see Ref. [29]). In Ref. [10] it was shown that even chiral nuclear potentials at

next-to-leading order (NLO), which are rather simplistic and contain no three-body forces, exhibit a correlation slope consistent with previous microscopic calculations at N2LO and N3LO in the chiral expansion. This suggests that certain aspects of the correlation are ultimately associated with low-energy physics well described even at next-to-leading order in the chiral expansion. In the present work we will demonstrate that this is indeed the case and that the slope of the correlation can be derived without referring to detailed properties of the nucleon-nucleon potential. The overall scale is then set by a few constants that can in principle be extracted from the properties of low-density homogeneous matter. We also show that the same arguments can be used to derive the slope of the correlation between the symmetry energy and its curvature at nuclear matter saturation density.

We take as a starting point the nuclear symmetry energy  $S(\rho)$ , which is defined as the difference in the energy per nucleon between neutron matter and symmetric nuclear matter at a given density:

$$S(\rho) = \frac{E}{N}(\rho, \delta_{np} = 1) - \frac{E}{N}(\rho, \delta_{np} = 0), \quad (1)$$

where  $\rho$  is the total baryon number density,  $N$  is the total baryon number, and  $\delta_{np} = (\rho_n - \rho_p)/(\rho_n + \rho_p)$  is the isospin asymmetry parameter. A Maclaurin expansion of the nuclear equation of state around symmetric nuclear matter

$$\frac{E}{N}(\rho, \delta_{np}) = \sum_{n=0}^{\infty} A_{2n}(\rho) \delta_{np}^{2n} \quad (2)$$

is in general [30, 31] nonconvergent due to the appearance of nonanalytic logarithm terms that appear beyond a mean field description of the nuclear equation of state:

$$\begin{aligned} \frac{E}{N}(\rho, \delta_{np}) = & A_0(\rho) + S_2(\rho) \delta_{np}^2 \\ & + \sum_{n=2}^{\infty} (S_{2n} + L_{2n} \ln |\delta_{np}|) \delta_{np}^{2n}. \end{aligned} \quad (3)$$

However, all contributions beyond the quadratic term  $S_2$ , which we call the isospin-asymmetry energy, have been

\*Electronic address: [holt@physics.tamu.edu](mailto:holt@physics.tamu.edu)

†Electronic address: [yylim@tamu.edu](mailto:yylim@tamu.edu)

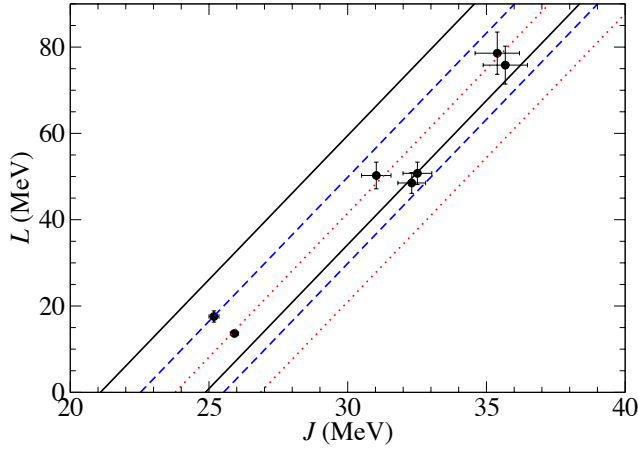


FIG. 1: (color online) Symmetry energy  $J$  vs. its slope parameter  $L$  from the seven chiral nuclear potentials considered in this work. The bands are obtained by keeping all terms up to  $a_0$  (red dotted),  $a_1$  (blue dashed), and  $a_2$  (black solid) in Eq. (11).

shown to be small at low temperatures when realistic nuclear forces are employed [31–37]. It is therefore a good approximation to identify the nuclear symmetry energy  $S(\rho)$  with the isospin-asymmetry energy  $S_2(\rho)$ . In practice it is the latter quantity that can be inferred from laboratory measurements of finite nuclei.

It is common to expand the density dependence of the isospin-asymmetry energy in a Taylor series around nuclear saturation:

$$S_2(\rho) = J + L \left( \frac{\rho - \rho_0}{3\rho_0} \right) + \frac{1}{2} K_{\text{sym}} \left( \frac{\rho - \rho_0}{3\rho_0} \right)^2 + \dots, \quad (4)$$

where  $J \equiv S_2(\rho_0)$ . The parameters  $L$  and  $K_{\text{sym}}$  can then be extracted from properties of finite nuclei [38], but their uncertainties are much larger than that associated with the isospin-asymmetry energy. For this reason correlations between the nuclear symmetry energy, the slope parameter, and curvature are routinely investigated within a range of theoretical models [7, 26–29, 39, 40].

In Fermi liquid theory the nuclear isospin-asymmetry energy is rigorously defined at all densities in terms of the isotropic component  $f'_0$  of the isovector-scalar quasiparticle interaction according to

$$S_2(\rho) = \frac{k_F^2}{6m^*} \left( 1 + \frac{2m^*k_F}{\pi^2} f'_0 \right), \quad (5)$$

where  $k_F$  is the Fermi momentum and the nucleon effective mass  $m^*$  is related to the Fermi liquid parameter  $f_1$  through

$$\frac{1}{m^*} = \frac{1}{m} - \frac{2k_F}{3\pi^2} f_1. \quad (6)$$

These Fermi liquid parameters are obtained by performing a Legendre polynomial decomposition of the central

quasiparticle interaction

$$\mathcal{F}(\vec{p}_1, \vec{p}_2) = \sum_l (f_l + g_l \vec{\sigma}_1 \cdot \vec{\sigma}_2 + f'_l \vec{\tau}_1 \cdot \vec{\tau}_2 + g'_l \vec{\sigma}_1 \cdot \vec{\sigma}_2 \vec{\tau}_1 \cdot \vec{\tau}_2) P_l(\cos \theta), \quad (7)$$

in the relative angle  $\cos \theta = \hat{p}_1 \cdot \hat{p}_2$ . Expanding Eq. (5) we obtain

$$S_2(\rho) = \frac{k_F^2}{6m} + \frac{k_F^3}{9\pi^2} [3f'_0(\rho) - f_1(\rho)]. \quad (8)$$

The relationship in Eq. (8) can be used to derive a correlation between the symmetry energy slope parameter  $L$  and the symmetry energy  $J$  at nuclear matter saturation density:

$$L = 3\rho_0 \left. \frac{dS_2}{d\rho} \right|_{\rho_0} = 3J - S_0 + \frac{\rho_0}{6} \left( 3k_F \frac{df'_0}{dk_F} - k_F \frac{df_1}{dk_F} \right) \Big|_{k_F^0}, \quad (9)$$

where  $\rho_0 = 0.16 \text{ fm}^{-3}$  is nuclear matter saturation density,  $k_F^0$  is the Fermi momentum at saturation density, and  $S_0 \equiv (k_F^0)^2/(6m)$  is the noninteracting part of the isospin-asymmetry energy at saturation density. To study the additional correlation between  $L$  and  $J$  associated with the density derivative terms on the right-hand side of Eq. (12), we perform a Taylor series expansion of the quantity  $3f'_0 - f_1$  around a small reference density set by  $k_F = k_r$ :

$$3f'_0(k_F) - f_1(k_F) = a_0 + a_1 \beta + \frac{1}{2} a_2 \beta^2 + \dots, \quad (10)$$

where  $\beta = (k_F - k_r)/k_r$ .

In principle the choice of reference Fermi momentum  $k_r$  is arbitrary, but we note several constraints. First, logarithmic contributions to the isospin-asymmetry energy of the form  $\log(1 + 4k_F^2/m_\pi^2)$  arise from the one-pion-exchange Fock diagram [41] and formally require that  $k_r \gtrsim 0.9 \text{ fm}^{-1}$  in order for the Taylor series to be convergent at nuclear matter saturation density. Second,  $k_r$  should be small enough that a reliable calculation of the Fermi liquid parameters  $f'_0(k_r)$  and  $f_1(k_r)$  may be achieved within chiral effective field theory whose formal expansion parameter at the reference density would be  $k_r/\Lambda_\chi$ , where  $\Lambda_\chi \sim 500 \text{ MeV}$  is a typical momentum-space cutoff scale in realistic chiral nucleon-nucleon potentials. The effect of the less certain three-body forces, which start contributing to the homogeneous matter equation of state at a density  $\rho \simeq 0.03 \text{ fm}^{-3}$  [42–44], should also be minimized. From these considerations we choose the reference Fermi momentum  $k_r = 0.9 \text{ fm}^{-1} = 175 \text{ MeV}$ , which satisfies  $(k_F^0 - k_r)/k_r \simeq 0.5$ , where  $k_F^0$  is the Fermi momentum of nuclear matter at saturation density. We will show later that this value, which corresponds to the density  $\rho \simeq 0.05 \text{ fm}^{-3}$ , is large enough that keeping the first three terms in the Taylor series expansion in Eq. (10) provides a good description of the

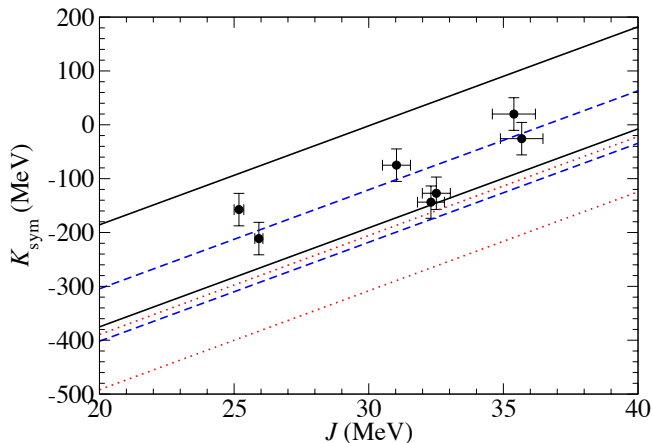


FIG. 2: (Color online) Symmetry energy  $J$  vs. its curvature parameter  $K_{\text{sym}}$  from the seven chiral nuclear potentials considered in this work. The bands are obtained by keeping all terms up to  $a_0$  (red dotted),  $a_1$  (blue dashed), and  $a_2$  (black solid) in Eq. (13).

isospin-asymmetry energy somewhat above nuclear saturation density, even though formally the series fails to converge in that regime.

Only the terms in Eq. (10) proportional to  $a_1$  and  $a_2$  result in additional correlations between  $L$  and  $J$ . Our strategy is therefore to absorb the dependence of the  $L$  vs.  $J$  correlation on the choice of nuclear interaction into the coefficient  $a_0$ , which we expect to be very similar for different nuclear force models. Combining Eqs. (10) and (12) and defining  $\gamma \equiv 2k_F^2/(k_F^2 - k_r^2)$ , we find the unique solution

$$L = (3 + \gamma)J - (1 + \gamma)S_0 - \gamma \frac{\rho_0}{6} (a_0 - \eta_1 a_1 + \eta_1 a_2), \quad (11)$$

where  $\eta_1 = (\beta + 1)\gamma^{-1} - \beta$ . This rearrangement simultaneously minimizes the residual importance of  $a_1$  and  $a_2$  after we have included their effect on the  $L$  vs.  $J$  correlation through the term  $(3 + \gamma)J$ . For instance, if  $k_r = 0.9 \text{ fm}^{-1}$ , then  $\gamma \simeq 3.7$  and  $\eta_1 \simeq -0.08$ . We therefore expect  $a_0$  to give the dominant contribution to the last term on the right-hand side of Eq. (11).

In Fig. 1 we show the values of the symmetry energy and its slope parameter at nuclear matter saturation density for a set of seven realistic nuclear potentials [45–48] at different orders in the chiral expansion and different values of the momentum-space cut-off  $\Lambda$ : {N1LO\_450, N1LO\_500, N2LO\_450, N2LO\_500, N3LO\_414, N3LO\_450, N3LO\_500}. Since the equation of state of pure neutron matter is well converged in many-body perturbation theory up to nuclear matter saturation density using modern chiral effective field theory forces with  $\Lambda \lesssim 500 \text{ MeV}$  [10], we compute in Fig. 1 the symmetry energy assuming a symmetric nuclear matter saturation density  $\rho = 0.155 - 0.165 \text{ fm}^{-3}$  and a saturation binding energy of  $E/N = 16 \text{ MeV}$ . The error

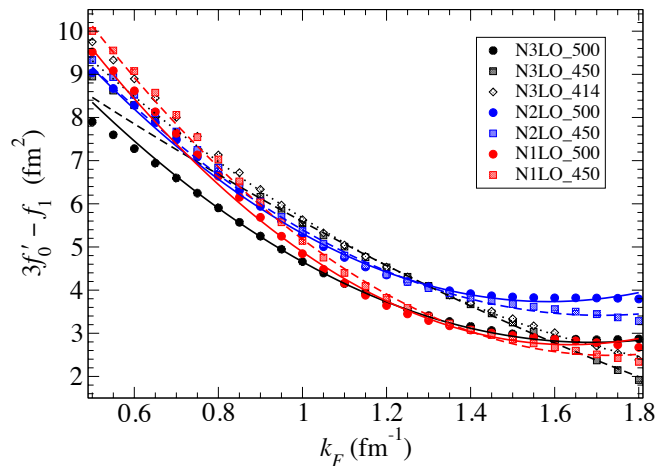


FIG. 3: (Color online) Combination of the Fermi liquid parameters associated with the isospin-asymmetry energy as a function of Fermi momentum. The solid lines are fit functions of the form given in Eq. (10) over the range  $0.85 \text{ fm}^{-1} < k_F < 1.8 \text{ fm}^{-1}$ .

bars on the data points arise from varying the saturation density within the above range. We can also extract the isospin-asymmetry energy directly from a calculation of the quasiparticle interaction in Fermi liquid theory starting from chiral two- and three-body forces as described in Refs. [49–52]. In Fig. 1 we show as well the correlation bands obtained by keeping in Eq. (11) only the  $a_0$  term (red-dotted lines), the  $a_0$  and  $a_1$  terms (blue-dashed lines), and all three terms  $a_0$ ,  $a_1$ , and  $a_2$  (black solid lines) by fitting the density-dependent isospin-asymmetry energy from Eqs. (8) and (10) over the range  $0.85 \text{ fm}^{-1} < k_F < 1.8 \text{ fm}^{-1}$  for each of the seven chiral nuclear forces considered in this work. We see that indeed the model-independent prediction for the slope of the  $J$  vs.  $L$  correlation,  $m_L \simeq 6.7$ , is well satisfied by all N1LO, N2LO, and N3LO chiral nuclear forces. We also observe that the size of the uncertainty band is set already from the uncertainties in  $a_0$  and that the inclusion of  $a_1$  and  $a_2$  leads primarily to a shift of the band.

We can extend this analysis to derive an additional correlation between the symmetry energy incompressibility  $K_{\text{sym}}$  and  $J$ :

$$K_{\text{sym}} = 9\rho_0^2 \left. \frac{d^2 S_2}{d\rho^2} \right|_{\rho_0} = 4L - 12J + 2S_0 + \frac{\rho_0}{6} \left( 3k_F^2 \frac{d^2 f'_0}{dk_F^2} - k_F^2 \frac{d^2 f_1}{dk_F^2} \right) \Big|_{k_F^0}. \quad (12)$$

By again minimizing the explicit dependence on  $a_1$  and  $a_2$  we obtain the unique solution

$$K_{\text{sym}} = 5\gamma J - (5\gamma + 2)S_0 - 5\gamma \frac{\rho_0}{6} (a_0 - \eta_2 a_1 + \eta_2 a_2), \quad (13)$$

where  $\eta_2 = 4(\beta + 1)\gamma^{-1} - 5\beta$ . Now for  $k_r = 0.9 \text{ fm}^{-1}$ , we obtain  $\eta_2 \simeq -0.16$  and therefore we expect the residual

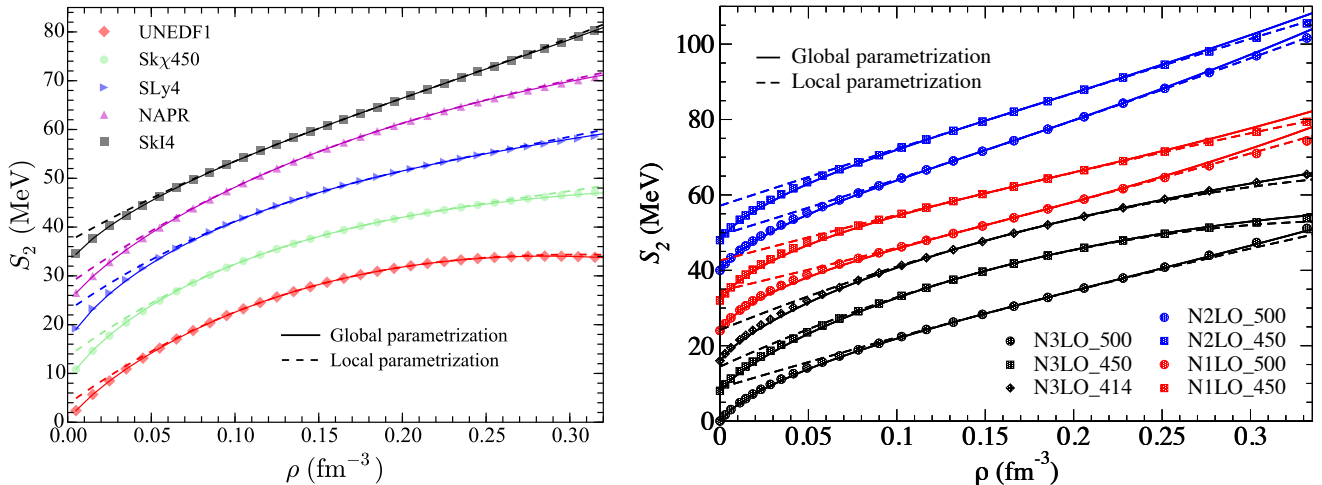


FIG. 4: (Color online) Left: nuclear isospin-asymmetry energy as a function of density from various Skyrme force models. Right: nuclear isospin-asymmetry energy as a function of density from various chiral nuclear forces. Note that in both figures we have introduced a vertical offset to better distinguish the different curves.

importance of  $a_1$  and  $a_2$  to be greater than in the  $L$  vs.  $J$  correlation. Nevertheless, we have derived a second universal slope parameter  $m_K = 5\gamma \simeq 18.4$  for the  $J$  vs.  $K_{\text{sym}}$  correlation that is independent of details of the nuclear force employed.

In Fig. 2 we show the values of the symmetry energy  $J$  and curvature  $K_{\text{sym}}$  at nuclear saturation density using the same set of chiral potentials. The largest source of uncertainty (represented by the error bars on the correlation points) is the assumed value the symmetric nuclear matter incompressibility  $K_0 = 220 - 260$  MeV [53, 54]. We show as well the correlation bands obtained by keeping in Eq. (13) only the  $a_0$  term (red-dotted lines), the  $a_0$  and  $a_1$  terms (blue-dashed lines), and all three terms  $a_0$ ,  $a_1$ , and  $a_2$  (black solid lines). Again we see that the slope of the correlation is well determined from our model-independent analysis and that the overall spread in the uncertainty band is set with the inclusion of only the  $a_0$  term in Eq. (13).

In Fig. 3 we show the Fermi momentum dependence of the quantity  $3f'_0(k_F) - f_1(k_F)$  for the seven chiral potentials considered in this work. We note that the N3LO\_500 chiral potential exhibits the poorest convergence in many-body perturbation theory, which may account for its different low-density behavior. When fitting the theoretical results with the functional form given in Eq. (10), we include only the points for which  $k_F > 0.85 \text{ fm}^{-1}$ . For smaller values of the Fermi momentum, we found that third-order perturbative contributions (not included explicitly in this work) become important. We see that indeed the functional form in Eq. (10) is able to well reproduce the Fermi momentum dependence of the Fermi liquid parameters up to  $k_F \simeq 1.8 \text{ fm}^{-1}$ . We find for the values of the expansion coefficients:  $a_0 = 5.88 \pm 0.35 \text{ fm}^2$ ,  $a_1 = -6.04 \pm 0.91 \text{ fm}^2$ , and  $a_2 = 6.08 \pm 2.48 \text{ fm}^2$  averaged over the seven chi-

ral potentials. Combined with the expansion parameter  $\beta = 0.5$ , we see that the explicit calculations suggest a convergent series at nuclear matter saturation density.

Finally we observe that the ansatz for the density dependence of the isospin-asymmetry energy in Eqs. (8) and (10) produces the first four terms in the general expansion

$$S_2(\rho) = \sum_{i=0}^N b_i \left( \frac{\rho}{\rho_0} \right)^{(i+2)/3}. \quad (14)$$

Combining Eq. (14) with the definition of the symmetry energy parameters in Eq. (4), we obtain

$$\begin{aligned} b_0 &= S_0, \\ b_1 &= \frac{1}{2} K_{\text{sym}} - 3L + 10J - 3S_0, \\ b_2 &= -K_{\text{sym}} + 5L - 15J + 3S_0, \\ b_3 &= \frac{1}{2} K_{\text{sym}} - 2L + 6J - S_0. \end{aligned} \quad (15)$$

These expressions are of course independent of the choice of reference Fermi momentum  $k_r$ . In Fig. 4 we show the accuracy of this global parametrization (solid lines) compared to the normal Taylor series expansion about nuclear saturation density (dashed lines) in Eq. (4). We show results for both a representative set of Skyrme mean field models (on the left) as well as the seven chiral interactions (on the right). We note that a vertical offset is used in order to separate the curves. In general the Taylor expansion in Eq. (4) does not reproduce well the low-density behavior of the isospin-asymmetry energy, especially in the case of chiral nuclear interactions. Each Skyrme force model contains a density-dependent interaction with corresponding contribution to the symmetry

energy

$$S_{2d}(\rho) = -\frac{t_3}{24} \left( \frac{1}{2} + x_3 \right) \rho^{1+\epsilon_1} - \frac{t_4}{24} \left( \frac{1}{2} + x_4 \right) \rho^{1+\epsilon_2}, \quad (16)$$

where  $t_i$  and  $x_i$  are independent of density. For example, UNEDF1 [55], SLy4 [56], NAPR [3], and SkI4 [57] have the values  $\epsilon_1 = \{0.27, 1/6, 0.1441, 1/4\}$ , while the Sk $\chi$ 450 [58] interaction has the two parameters  $\epsilon_1 = 1/3, \epsilon_2 = 1$ . Thus, the fitting function in Eqs. (14) and (15) is quite flexible, and we suggest that it may provide a more useful global parametrization of the nuclear isospin-asymmetry energy.

In summary we have derived correlations between the nuclear isospin-asymmetry energy, its slope parameter, and curvature within a Fermi liquid theory description

of nuclear matter. We derived universal slope parameters for the  $J$  vs.  $L$  and  $J$  vs.  $K_{\text{sym}}$  correlations that are nearly independent of details of the nuclear interaction. We have assumed only that the quasiparticle interaction in nuclear matter at the low density scale set by  $k_F = k_r = 0.9 \text{ fm}^{-1}$  should be well described by any realistic nucleon-nucleon potential fitted to scattering phase shifts. Future efforts to reduce the theoretical uncertainties on the Fermi liquid parameters at this low-density scale may then give more stringent constraints on the symmetry energy correlation curves.

## Acknowledgments

Work supported by the National Science Foundation under grant No. PHY1652199.

- 
- [1] J. M. Lattimer and M. Prakash, Phys. Rept. **333-334**, 121 (2000).
- [2] J. M. Lattimer and M. Prakash, Astrophys. J. **550**, 426 (2001).
- [3] A. W. Steiner, M. Prakash, J. M. Lattimer, and P. Ellis, Phys. Rept. **411**, 325 (2005).
- [4] J. M. Lattimer and Y. Lim, Astrophys. J. **771**, 51 (2013).
- [5] A. Steiner and S. Gandolfi, Phys. Rev. Lett. **108**, 081102 (2012).
- [6] S. Gandolfi, J. Carlson, and S. Reddy, Phys. Rev. C **85**, 032801 (2012).
- [7] C. Xu, B.-A. Li, and L.-W. Chen, Phys. Rev. C **82**, 054607 (2010).
- [8] M. Kortelainen, T. Lesinski, J. Moré, W. Nazarewicz, J. Sarich, N. Schunck, M. V. Stoitsov, and S. Wild, Phys. Rev. C **82**, 024313 (2010).
- [9] K. Hebeler, J. M. Lattimer, C. J. Pethick, and A. Schwenk, Phys. Rev. Lett. **105**, 161102 (2010).
- [10] J. W. Holt and N. Kaiser, Phys. Rev. C **95**, 034326 (2017).
- [11] D. V. Shetty, S. J. Yennello, and G. A. Souliotis, Phys. Rev. C **76**, 024606 (2007).
- [12] M. B. Tsang, Y. Zhang, P. Danielewicz, M. Famiano, Z. Li, W. G. Lynch, and A. W. Steiner, Phys. Rev. Lett. **102**, 122701 (2009).
- [13] M. Centelles, X. Roca-Maza, X. Viñas, and M. Warda, Phys. Rev. Lett. **102**, 122502 (2009).
- [14] L.-W. Chen, C. M. Ko, B.-A. Li, and J. Xu, Phys. Rev. C **82**, 024321 (2010).
- [15] A. Carbone, G. Colò, A. Bracco, L.-G. Cao, P. F. Bortignon, F. Camera, and O. Wieland, Phys. Rev. C **81**, 041301 (2010).
- [16] X. Roca-Maza, M. Centelles, X. Viñas, and M. Warda, Phys. Rev. Lett. **106**, 252501 (2011).
- [17] X. Viñas, M. Centelles, X. Roca-Maza, and M. Warda, Eur. Phys. J. A **50**, 27 (2014).
- [18] P.-G. Reinhard and W. Nazarewicz, Phys. Rev. C **81**, 051303 (2010).
- [19] A. Tamii *et al.*, Phys. Rev. Lett. **107**, 062502 (2011).
- [20] J. Piekarewicz, B. K. Agrawal, G. Colò, W. Nazarewicz, N. Paar, P.-G. Reinhard, X. Roca-Maza, and D. Vretenar, Phys. Rev. C **85**, 041302 (2012).
- [21] X. Roca-Maza, X. Viñas, M. Centelles, B. K. Agrawal, G. Colò, N. Paar, J. Piekarewicz, and D. Vretenar, Phys. Rev. C **92**, 064304 (2015).
- [22] T. Hashimoto *et al.*, Phys. Rev. C **92**, 031305 (2015).
- [23] A. Tonchev, N. Tsoneva, C. Bhatia, C. Arnold, S. Goriely, S. Hammond, J. Kelley, E. Kwan, H. Lenske, J. Piekarewicz, R. Raut, G. Rusev, T. Shizuma, and W. Tornow, Phys. Lett. B **773**, 20 (2017).
- [24] B. A. Brown, Phys. Rev. Lett. **119**, 122502 (2017).
- [25] J. Yang and J. Piekarewicz, Phys. Rev. C **97**, 014314 (2018).
- [26] I. Vidaña, C. m. c. Providência, A. Polls, and A. Rios, Phys. Rev. C **80**, 045806 (2009).
- [27] C. Ducoin, J. Margueron, C. m. c. Providência, and I. Vidaña, Phys. Rev. C **83**, 045810 (2011).
- [28] B. M. Santos, M. Dutra, O. Lourenço, and A. Delfino, Phys. Rev. C **90**, 035203 (2014).
- [29] I. Tews, J. M. Lattimer, A. Ohnishi, and E. E. Kolomeitsev, Astrophys. J. **848**, 105 (2017).
- [30] N. Kaiser, Phys. Rev. C **91**, 065201 (2015).
- [31] C. Wellenhofer, J. W. Holt, and N. Kaiser, Phys. Rev. C **93**, 055802 (2016).
- [32] I. Bombaci and U. Lombardo, Phys. Rev. C **44**, 1892 (1991).
- [33] C.-H. Lee, T. T. S. Kuo, G. Q. Li, and G. E. Brown, Phys. Rev. C **57**, 3488 (1998).
- [34] W. Zuo, I. Bombaci, and U. Lombardo, Phys Rev C **60**, 024605 (1999).
- [35] W. Zuo, A. Lejeune, U. Lombardo, and J. F. Mathiot, Eur. Phys. J. A **14**, 469 (2002).
- [36] T. Frick, H. Müther, A. Rios, A. Polls, and A. Ramos, Phys. Rev. C **71**, 014313 (2005).
- [37] C. Drischler, V. Somà, and A. Schwenk, Phys. Rev. C **89**, 025806 (2014).
- [38] M. Dutra, O. Lourenço, J. S. Sá Martins, A. Delfino, J. R. Stone, and P. D. Stevenson, Phys. Rev. C **85**, 035201 (2012).
- [39] L.-W. Chen, B.-J. Cai, C. M. Ko, B.-A. Li, C. Shen, and J. Xu, Phys. Rev. C **80**, 014322 (2009).
- [40] P. Danielewicz and J. Lee, Nuclear Physics A **818**, 36 (2009).
- [41] N. Kaiser, Nucl. Phys. **A697**, 255 (2002).



- [42] K. Hebeler and A. Schwenk, *Phys. Rev. C* **82**, 014314 (2010).
- [43] G. Wlazłowski, J. W. Holt, S. Moroz, A. Bulgac, and K. Roche, *Phys. Rev. Lett.* **113**, 182503 (2014).
- [44] I. Tews, S. Gandolfi, A. Gezerlis, and A. Schwenk, *Phys. Rev. C* **93**, 024305 (2016).
- [45] D. R. Entem and R. Machleidt, *Phys. Rev. C* **68**, 041001 (2003).
- [46] L. Coraggio, J. W. Holt, N. Itaco, R. Machleidt, and F. Sammarruca, *Phys. Rev. C* **87**, 014322 (2013).
- [47] L. Coraggio, J. W. Holt, N. Itaco, R. Machleidt, L. E. Marcucci, and F. Sammarruca, *Phys. Rev. C* **89**, 044321 (2014).
- [48] F. Sammarruca, L. Coraggio, J. W. Holt, N. Itaco, R. Machleidt, and L. E. Marcucci, *Phys. Rev. C* **91**, 054311 (2015).
- [49] J. W. Holt, N. Kaiser, and W. Weise, *Nucl. Phys.* **A870-871**, 1 (2011).
- [50] J. W. Holt, N. Kaiser, and W. Weise, *Nucl. Phys.* **A876**, 61 (2012).
- [51] J. W. Holt, N. Kaiser, and W. Weise, *Phys. Rev. C* **87**, 014338 (2013).
- [52] J. W. Holt, N. Kaiser, and T. R. Whitehead, arXiv:1712.05013 (2017).
- [53] D. H. Youngblood, H. L. Clark, and Y.-W. Lui, *Phys. Rev. Lett.* **82**, 691 (1999).
- [54] S. Shlomo, V. M. Kolomietz, and G. Colò, *Eur. Phys. J. A* **30**, 23 (2006).
- [55] M. Kortelainen, J. McDonnell, W. Nazarewicz, P.-G. Reinhard, J. Sarich, N. Schunck, M. V. Stoitsov, and S. M. Wild, *Phys. Rev. C* **85**, 024304 (2012).
- [56] E. Chabanat, P. Bonche, P. Haensel, J. Meyer, and R. Schaeffer, *Nucl. Phys.* **A635**, 231 (1998).
- [57] P.-G. Reinhard and H. Flocard, *Nucl. Phys.* **A584**, 467 (1995).
- [58] Y. Lim and J. W. Holt, *Phys. Rev. C* **95**, 065805 (2017).